Front. Earth Sci. 2024, 18(2): 312–323
https://doi.org/10.1007/s11707-022-1064-4

RESEARCH ARTICLE

Changes of tropical cyclone size in three oceanic basins of the northern hemisphere from 2001 to 2021

Banglin ZHANG (✉)[1,2], Jeremy Cheuk-Hin LEUNG[1], Shengyuan LIU[1,3], Jianjun XU[4]

1 Guangzhou Institute of Tropical and Marine Meteorology/Guangdong Provincial Key Laboratory of Regional Numerical Weather Prediction, CMA, Guangzhou 510640, China
2 College of Atmospheric Science, Lanzhou University, Lanzhou 730020, China
3 College of Ocean and Meteorology, Guangdong Ocean University, Zhanjiang 524088, China
4 CMA-GDOU Joint Laboratory for Marine Meteorology & South China Sea Institute of Marine Meteorology, Guangdong Ocean University, Zhanjiang 524088, China

Abstract In this study the changes of tropical cyclone (TC) size from 2001 to 2021 are analyzed based on linear and quadratic curve fittings of the National Hurricane Center (NHC) / Joint Typhoon Warning Center (JTWC) best track data, based on the radius of maximum wind (RMW) and the average radius of 34-kt wind (AR34), in three oceanic basins of the North Atlantic (NATL), the Western North Pacific (WPAC) and the Eastern North Pacific (EPAC). The computations are done separately for two categories of tropical cyclones: tropical storms (TS) and hurricanes (HT). Size changes of landfalling and non-landfalling TCs are also discussed. Results show that there is a great inter-basin variability among the changes in TC sizes. Major conclusions include: 1) overall, the inner cores of TSs have become larger in all three basins, with the increasing tendencies being significant in the NATL and WAPC, while those of HTs mostly get smaller or remain similar; 2) meanwhile, comparatively large inter-basin differences are observed for the TC outer core sizes, and the sizes of landfalling TCs; 3) particularly, a significant decrease in landfalling HT outer core size is observed over the EPAC; 4) in contrast, significant increases in landfalling TS inner core size are found over the NATL and WPAC. The presented analysis results could benefit future research about TC forecasts, storm surge studies, and the cyclone climate and its changes.

Keywords tropical cyclone, storm size, frequency, intensity, duration

Received August 31, 2022; accepted November 14, 2022

E-mail: zhangbl@gd121.cn

1 Introduction

Tropical cyclones are a major source of natural catastrophic losses worldwide. It is estimated that 10000 people have died every year since 1980 due to tropical cyclones (Doocy et al., 2013), and thus it is of great importance to study tropical cyclones and to understand their response to changes in environmental conditions such as sea surface temperature (SST).

In past decades, the sensitivity of frequency, intensity, and duration of tropical cyclones to climate change has been extensively investigated with a general conclusion that both global and regional changes in TC behavior should be expected as the climate and SST change (e.g., Klotzbach, 2006; Emanuel et al., 2008; Martinez-Sanchez and Cavazos, 2014; Jin et al., 2014; Kossin, 2017). Though numerous studies have examined the complex response of tropical cyclone frequency and intensity to climate change (Emanuel, 2005; Webster et al., 2005; Shen, 2006; Emanuel et al., 2008; Barbosa, 2011; Emanuel and Sobel, 2013; Mei et al., 2015; Kossin, 2017). For example, Webster et al. (2005) found that both the number and percentage of global category 4–5 hurricanes increased significantly from 1970 to 2004; however, Klotzbach and Landsea (2015) found an insignificant downward trend in global frequency of category 4–5 hurricanes from 1990 to 2014, which may be because of the insignificant trend of global accumulated cyclone energy (ACE) despite warming SSTs (Klotzbach, 2006). Other studies have examined the variation of "storm days", namely the number of days in a season/year that a tropical cyclone exists, generally finding significant interdecadal variability. Landsea et al. (1999) was one of the earliest studies to note this, documenting a greater degree of statistical significance in storm days than in

hurricane frequency from 1944 to 1996. With updated data, Webster et al. (2005) and Wang et al. (2010) similarly found a large-amplitude fluctuation in storm days that was regulated by El Niño / Southern Oscillation (ENSO) and the Pacific Decadal Oscillation (PDO). Like previous studies, they did not find a linear trend, suggesting that the rising temperature so far has not yet had an impact on the global total number of storm days.

In this report we focus on changes in storm size, a relatively understudied topic. A major motivation for this work is that storm size can significantly impact damage, particularly that caused by storm surge (e.g., Irish et al., 2008; Grinsted et al., 2012), in addition to storm intensity. For example, hurricanes Katrina (2005) and Ike (2008) which are characterized with large storm size brought more severe storm surge than other TCs that have similar intensity, which has been discussed in Klotzbach et al. (2020) and Irish et al. (2008), etc. Thus, the storm size is an essential parameter when estimating storm (surge) damages (e.g., Islam et al., 2021). Another motivation is that storm size impacts predictability; large storms tend to evolve more slowly and are more predictable than small storms (Carrasco et al., 2014). A number of previous studies have investigated the climatology of storm size. For example, the radius of the outermost closed isobar (ROCI) was used to examine the climatology and structure of tropical cyclones of different sizes (Merrill, 1984). A climatology with multiple tropical cyclone size parameters for the North Atlantic basin was then established with data from 1988 through 2002 (Kimball and Mulekar, 2004). Recently the Quick Scatterometer (QuikSCAT) surface wind speed estimates and storm-centered infrared data were also used to estimate the climatology of storm size (Chavas and Emanuel, 2010; Knaff et al., 2014; Chan and Chan, 2015).

Recently, there have been some studies documenting the observed trends in storm size over different basins in the past years, despite the limited sampling size and data availability. For example, Nekkali et al. (2022) showed an increase in R34 of TCs over the Bay of Bengal region from 2002–2019. Shou et al. (2021), based on a new index of storm size, reported a significant decreasing trend of inner core size of Western North Pacific TCs. Islam et al. (2022) documented an increase in TC size during landfall which, together with the increasing intensity, led to the stronger storm surge in Japan from 1980 to 2009. Lin et al. (2015) suggested that TC size is more strongly related to the departure of local SST from area mean than it is to the SST anomaly from temporal average (SSTA). In independent research, it is reported that TC inner-core sizes mainly depend on the initial vortex size, which may be related to the moisture and surface energy flux conditions, based on numerical simulation experiments (Xu and Wang, 2010a,b).

Despite a number of previous studies, the characteristics of changes in storm size by considering the northern hemisphere as a whole are unclear. Thus, aiming at exploring the similarity and differences of storm size changes across different basins in the northern hemisphere, this study examines the inter-basin variability of changes in both the inner- and outer-core sizes of TC over the North Atlantic (NATL), the Western North Pacific (WPAC) and the Eastern North Pacific (EPAC) from 2001 to 2021, where more reliable storm size data are available. The remainder of this study proceeds as follows. The size data and the analytic method for diagnosing the changes in storm size are described in Section 2. The results are present in Section 3, and Section 4 summarizes the findings and presents some discussions.

2 Data and methods

This research examines the characteristics and changes in storm size, collectively in the NATL, WPAC, and EPAC, and also individually in each basin. The initial focus is on 2001–2021, which corresponds to the period when TC size information is available for all the three basins. Longer-term NATL and WPAC data sets are then interrogated to show tendencies in individual basins within a larger context. Emphasis is placed on results that are statistically significant with 90% confidence based on the linear tendencies. The details of the data and methods applied in this study is given below. It is noted here that because of the short record of the storm size data, we use the term linear tendency instead of linear trend to avoid confusions.

Making use of the International Best Track Archive for Climate Stewardship (IBTrACS; Knapp et al., 2010) data set (version 4, v04r00), we examine how TC size in NATL, EPAC, and WPAC had evolved from 2001 to 2021, based on the reported TC radius data. In the following study, the TC analyses over the NATL and EPAC were carried out based on the IBTrACS records provided by the National Hurricane Center (NHC), which is consistent with the best-track (i.e., b-decks) data sets are used from NHC and contain careful estimates of TC position, intensity, and size (Demuth et al., 2006; Landsea et al., 2010; Landsea and Franklin, 2013). The TC analyses over the WPAC were carried out based on the IBTrACS records provided by the Joint Typhoon Warning Center (JTWC). It is noted that the IBTrACS data does not include size information of TCs in the NATL and EPAC before 2004. Thus, for the size data over the NATL and EPAC basins from 2001 to 2003, we turned to the extended best track (EBT) data set (available at Regional and Mesoscale Meteorology Branch website) from the National Environmental Satellite, Data, and Information Service / Regional and Mesoscale Meteorology Branch (NESDIS/RAMMB) (Demuth et al. 2006), which uses the NHC best-track postanalysis when possible, but uses operational size estimates for earlier

storms. The operational size estimates are available from 1988 to 2003 for the NATL and 2001–2003 for the EPAC. Thus, this study focuses on the period 2001–2021, in which TC size data are available for all the three basins. It is remarked that the operational size estimates have not undergone the same level of quality control as those in the best-track archives (i.e., IBTrACS).

To define the size of a TC, we make use of the RMW and the 34-knot wind radius ($R34$) obtained from the above data sets, for the size of the TC inner and outer cores, respectively. The RMW gives a sense of the compactness of the inner core, whereas $R34$ demonstrates the breadth of the wind field. The JTWC and NHC provide $R34$ records of different quadrants, including the north-eastern, south-eastern, south-western, and north-western quadrants of a TC. For simplicity, we take averages of the four-quadrant $R34$ to indicate the mean radius of 34-knot wind radius of a TC (hereafter $AR34$). If the $R34$ of a particular quadrant has a 0 value, it is considered as a missing value and is not included in the averaging calculation. The TC size is presented by two metrics: 1) the TC radius (i.e., RMW and $AR34$), and 2) the TC area, derived from the TC radius by assuming the TC is a perfect circle (Eq. (1)). The TC areas derived based on RMW and $AR34$ are denoted as Area_{RMW} and Area_{AR34}, respectively. Since TCs are not perfect circles in reality, we also estimate the TC sizes by regarding TCs are ellipses, of which the semi-major and semi-minor axes are determined by the averages of two diagonal quadrant $R34$ (Eq. (2)). Note that quadrant radius records are available only for $R34$, so Eq. (2) is applied to $R34$ (denoted as Area'_{AR34}) but not to RMW. All these metrics (i.e., TC radius, TC area based on circle and ellipse area formulas) give consistent results of the changes in TC size from 2001 to 2021. It is remarked here that directly applying the RMW (or $R34$) from the data sets may cause uncertainty in the time series analyses, other methods have been proposed to reduce the uncertainty problem (e.g., Shou et al., 2021):

$$\begin{cases} \mathrm{Area}_{RMW} = \pi \times RMW^2 \\ \mathrm{Area}_{AR34} = \pi \times AR34^2 \end{cases}, \tag{1}$$

$$\mathrm{Area}'_{AR34} = \pi \times \frac{R34_{\mathrm{NE}} + R34_{\mathrm{SW}}}{2} \times \frac{R34_{\mathrm{NW}} + R34_{\mathrm{SE}}}{2}. \tag{2}$$

In the following analyses, all TC samples are categorized into three types according to the maximum sustained wind speed ($V_{\max}$): 1) TCs with $V_{\max} \geqslant 64$ kt, i.e., hurricanes / typhoons (denoted as HT), 2) TCs with 34 kt $\leqslant V_{\max} <$ 64 kt (denoted as tropical storms or TS), and 3) TCs with $V_{\max} \geqslant 34$ kt (denoted as ALL). Yearly storm size series are calculated by averaging the TC radius (i.e., RMW or $AR34$) or area (i.e., Area_{RMW} or Area_{AR34} or Area'_{AR34}) of all time points where the TC $V_{\max}$ fulfil the threshold. In other words, each time point with $V_{\max}$ meeting the threshold criteria is considered as one sample of the year. Storm sizes of landfalling and non-landfalling TCs are also examined, where landfalling TCs are regarded as those that made landfall at least once within their lifetime. The number of storm days is defined as the number of days with TC recorded each year. TC size over land were excluded in our analyses. Linear and quadratic curves (McDonald, 2014) are fit to all time series with the linear equation (Eq. (3)) and the quadratic equation (Eq. (4)), of which the former indicates the linear changes of the time series and the latter indicates the nonlinear changes characterized with apparent second derivatives or interdecadal variability:

$$Y = aX + b, \tag{3}$$

$$Y = aX^2 + bX + c, \tag{4}$$

where, X is time in yearly index. The two-tailed Students t-test is used to check if the linear tendencies of each time series are statistically significant.

Finally, the storm size derived from the best track cyclone data (available at JMA website) by Japan Meteorological Agency (JMA) RSMC Tokyo - Typhoon Center were also used for comparison (Kishimoto, 2008; Takagi and Wu, 2016) over the WPAC from 1977 to 2020. The JMA data set covers the period from 1951 to 2020, but size parameters are not available until 1977. One set of parameters are the longest and shortest radii of 50 kt winds or greater ($R50_{\mathrm{L}}$ and $R50_{\mathrm{S}}$), and another set of parameters are the longest and shortest radii of 30kt winds or greater ($R30_{\mathrm{L}}$ and $R30_{\mathrm{S}}$). Similarly, we derive the average $R50$ ($AR50$) and $R30$ ($AR30$) by taking averages of the longest and shortest radii. And, the TC area based on $R50$ and $R30$ are defined by Eq. (5) and Eq. (6), following Eq. (1) and Eq. (2), respectively:

$$\begin{cases} \mathrm{Area}_{AR30} = \pi \times AR30^2 \\ \mathrm{Area}_{AR50} = \pi \times AR50^2 \end{cases}, \tag{5}$$

$$\begin{cases} \mathrm{Area}'_{AR30} = \pi \times R30_{\mathrm{L}} \times R30_{\mathrm{S}} \\ \mathrm{Area}'_{AR50} = \pi \times R50_{\mathrm{L}} \times R50_{\mathrm{S}} \end{cases}. \tag{6}$$

3 Results

3.1 Storm days (SD)

Figure 1(a) gives the SD statistics averaged over the three basins from 2001 to 2021, for TS, HT, and ALL storms. For the three-basin average, only the SD of TS exhibits a significant increasing tendency (+12.75 days/decade, 99.9% confident), while those of HT and ALL are statistically insignificant (Fig. 1(a)). Meanwhile, the per-basin results reveal the unique characteristics of each basin. The WPAC has the highest percentage of strong storms, as indicated by the fact that HT storm days are

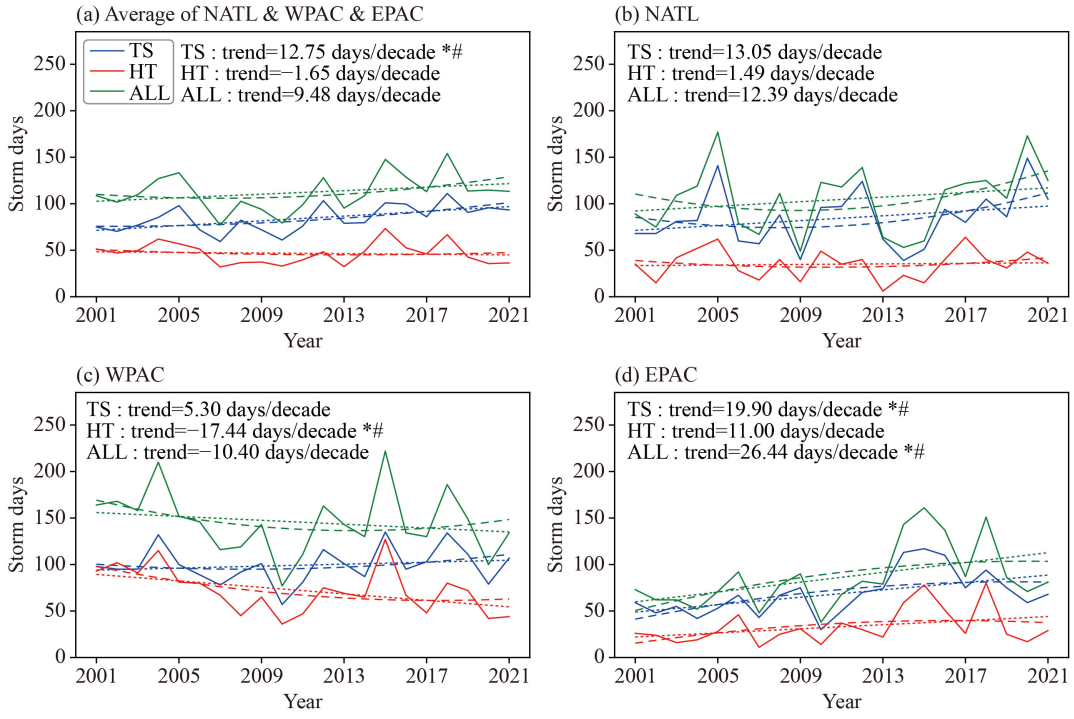

Fig. 1 Time series of the storm days (a) averaged over the three basins, and over the (b) NATL, (c) WPAC, and (d) EPAC from 2001 to 2021. The blue, red, and green solid curves indicate the TS, HT, and ALL storms, respectively. Dotted and dashed lines respectively show the best fit linear and quadratic tendencies. The linear tendency values are shown in the figure legends, with the asterisk (*) and hashtag (#) symbols denoting linear and quadratic fittings that are statistically significant with at least 90% confidence level.

almost equal to those of TS (Fig. 1(c)). In addition, the WPAC has the most total storm days for ALL storms. Among the three basins, the NATL exhibits statistically insignificant decreasing tendencies in SD (Fig. 1(b)), while the WPAC shows opposite long-term tendencies in SD between TS (+ 5.30 days/decade, insignificant) and HT (−17.4 days/decade, 95% confident) (Fig. 1(c)). The only basin with increasing SD tendencies in all TC categories is the EPAC, where the positive tendencies of all three categories range from 11.0 to 26.4 days/decade (Fig. 1(d)).

3.2 Changes in storm sizes for all TCs

In Fig. 2 we first examine the TC size variability from 2001 to 2021 averaged over all three examined basins. The general characteristics of the data, with HT having much larger *AR*34 and much smaller *RMW*, are consistent with the knowledge that mature storms are larger but have more compact inner cores (Shen, 2006). Significant positive tendencies of *RMW* are observed for both TS and ALL, with their values of 4.94 and 3.57 nm/decade, respectively. Meanwhile, that of HT (−0.04 nm/decade) does not pass the significance test (Fig. 2(a)). For *AR*34, statistically insignificant tendencies are observed for both HT (−3.16 nm/decade) and TS (+2.76 nm/decade) (Fig. 2(b)). As a result, averaging over the three basins, only Area_{MWR} of TS shows a statistically significant tendency (+1255.53 nm^2/decade) while others do not pass the significance test (Figs. 2(c)–2(e)).

Figures 3−4 demonstrate the time series of TC sizes over different basins, showing a great inter-basin variability. The *RMW*, for example, has generally a much larger increasing tendency in the NATL than in the WPAC and EPAC (Fig. 3). Meanwhile, *AR*34 in the EPAC decreases gradually when those in the NATL and WPAC do not change much (Fig. 4). As for the tendencies, the *RMW* of TS has increased over all the three basins, though that for HT varies by basin (Fig. 3), and the *RMW* tendencies are significant only in the NATL and WPAC. Specifically, in the NATL, the inner core radius of TS (+7.78 nm/decade) has increased significantly and but that of HT show an insignificant linear change (Fig. 3(a)). In the EPAC, the *RMW* tendencies for HT and TS oppose each other, but both of them are statistically insignificant (Fig. 3(c)). In WPAC, the increasing TS *RMW* is statistically significant (+4.37 nm/decade) but that of HT decreases significantly (−2.21 nm/decade) (Fig. 3(b)). Meanwhile, the tendency of AR34 for HT is insignificant in NATL (Fig. 4(a)), significantly positive in WPAC (+8.11 nm/decade, Fig. 4(b)), and significantly negative in EPAC (−15.0 nm/decade, Fig. 4(c)).

Consequently, for the NATL, increases in inner core areas are observed for TS but no apparent changes for its outer core; the size of HT also shows no significant

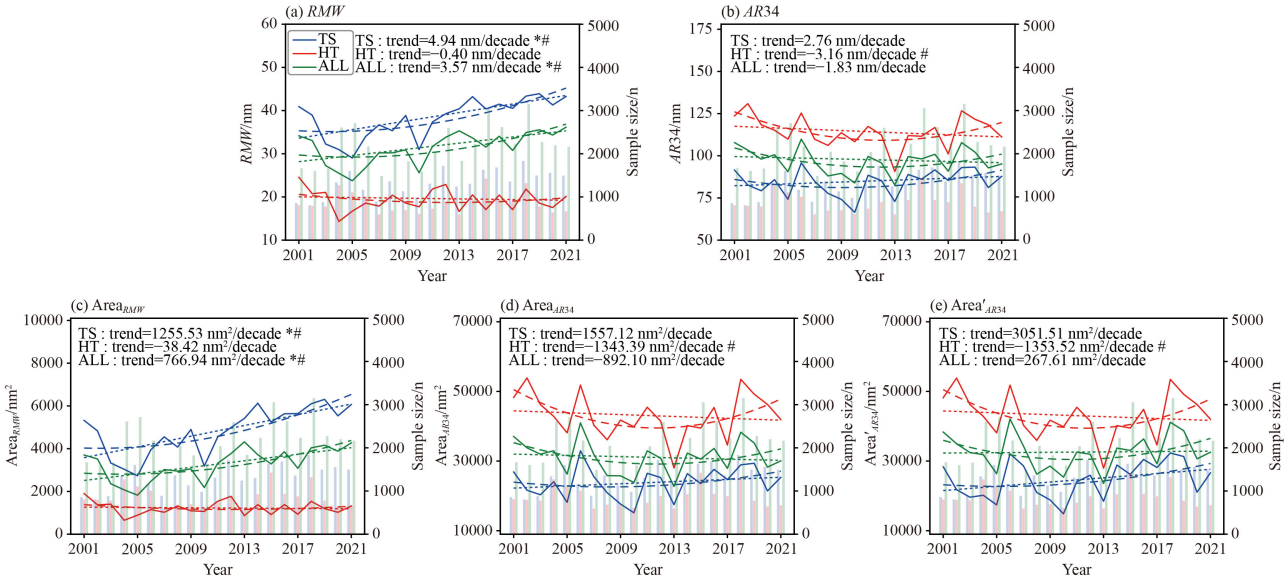

Fig. 2 Time series of the (a) *RMW* (unit: nm), (b) *AR*34 (unit: nm), (c) Area_{MWR} (unit: nm^2), (d) Area_{AR34} (unit: nm^2), and (e) Area'_{AR34} (unit: nm^2) from 2001 to 2021 averaged over the three basins. The blue, red, and green solid curves indicate the TS, HT, and ALL storms, respectively. Dotted and dashed lines respectively show the best fit linear and quadratic tendencies. The blue, red, and green bars indicate the sample sizes of the TS, HT, and ALL storms of each year. The linear trend tendencies are shown in the figure legends, with the asterisk (*) and hashtag (#) symbols denoting linear and quadratic fittings that are statistically significant with at least 90% confidence level.

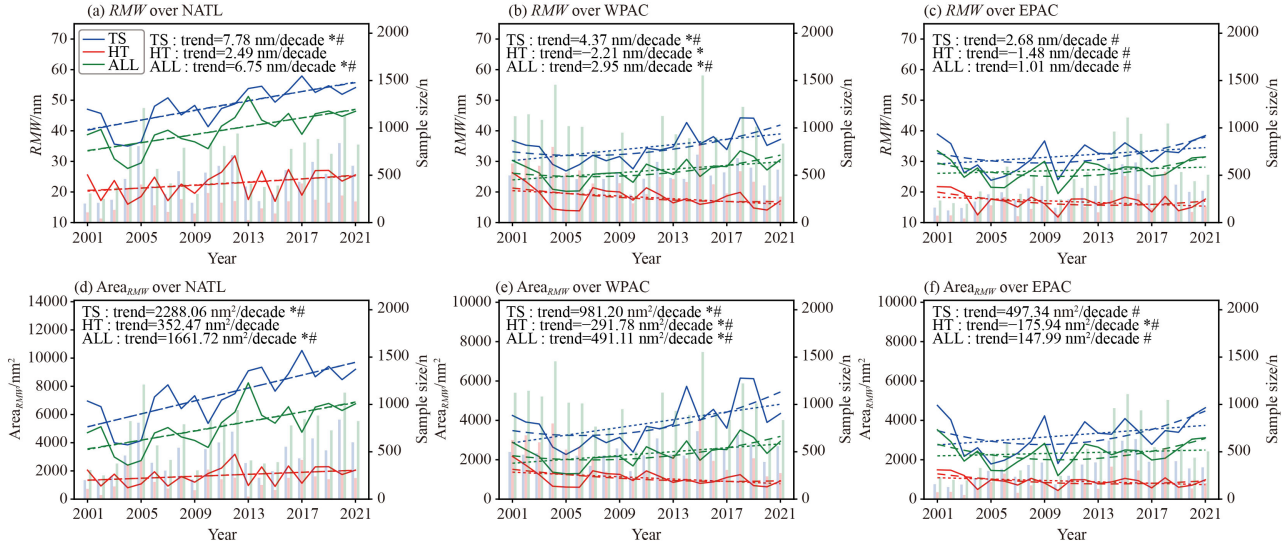

Fig. 3 (a)–(c) Time series of the *RMW* (unit: nm) from 2001 to 2021 over the (a) NATL, (b) WPAC and (c) EPAC, respectively. (d)–(f) Same as (a)–(c), except of the Area_{MWR} (unit: nm^2). The blue, red, and green solid curves indicate the TS, HT, and ALL storms, respectively. Dotted and dashed lines respectively show the best fit linear and quadratic tendencies. The blue, red, and green bars indicate the sample sizes of the TS, HT, and ALL storms of each year. The linear tendency values are shown in the figure legends, with the asterisk (*) and hashtag (#) symbols denoting linear and quadratic fittings that are statistically significant with at least 90% confidence level.

changes (Figs. 3(d), 4(d), and 4(g)). For the WPAC, both the inner and outer cores has expanded significantly for both the TS and HT since 2001 (Figs. 3(e), 4(e), and 4(h)). For the EPAC, the HT has been becoming smaller in both its inner and outer cores, but insignificant changes are observed for the TS (Figs. 3(f), 4(f), and 4(i)).

In addition to linear tendencies, we have also examined quadratic tendencies, which might better highlight decadal-scale forcing in the individual basins. The quadratic fitting for all parameters shows a large increase in statistical significance in both EPAC and WPAC, but not in the NATL. In fact, in the EPAC, all parameters have a significant quadratic tendency. This is likely indicative of the more pronounced decadal forcing

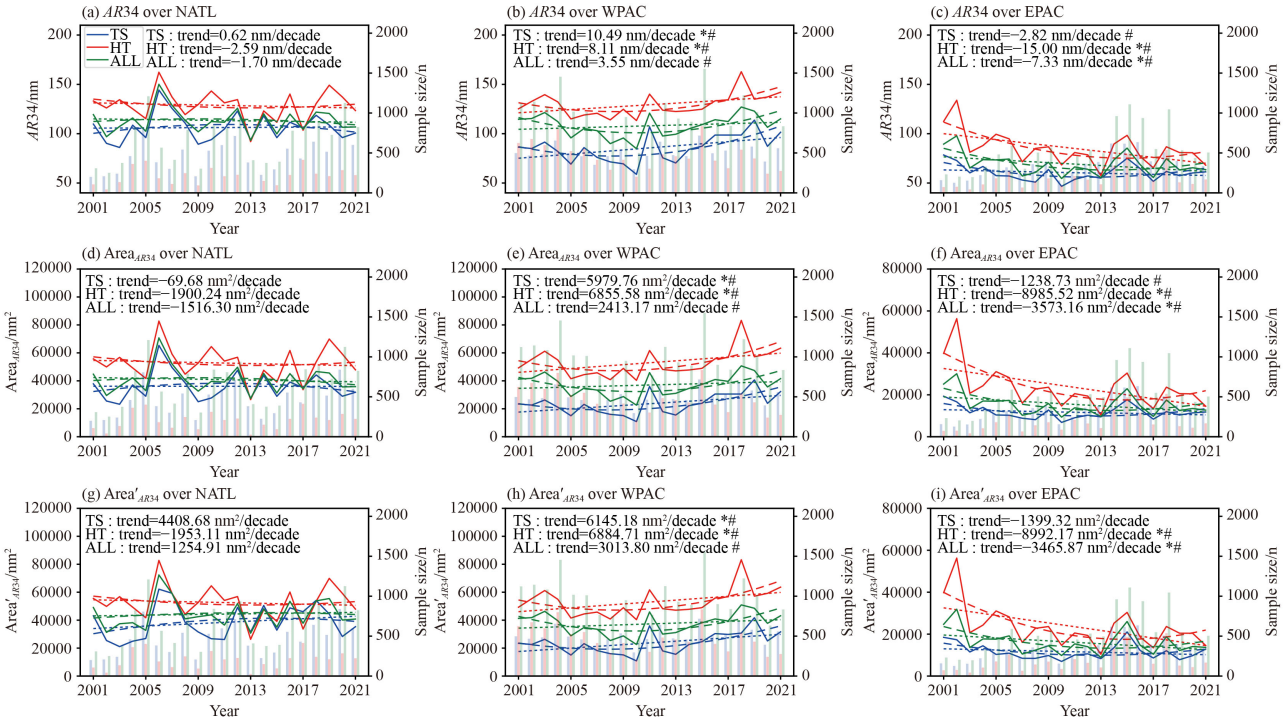

Fig. 4 (a)–(c) Time series of the AR34 (unit: nm) from 2001 to 2021 over the (a) NATL, (b) WPAC and (c) EPAC, respectively. (d)–(f) Same as (a)–(c), except of the Area$_{AR34}$ (unit: nm^2). (g)–(i) Same as (a)–(c), except of the Area′$_{AR34}$ (unit: nm^2). The blue, red, and green solid curves indicate the TS, HT, and ALL storms, respectively. Dotted and dashed lines respectively show the best fit linear and quadratic tendencies. The blue, red, and green bars indicate the sample sizes of the TS, HT, and ALL storms of each year. The linear tendency values are shown in the figure legends, with the asterisk (*) and hashtag (#) symbols denoting linear and quadratic fittings that are statistically significant with at least 90% confidence level.

(perhaps of SST) in the Pacific basins than in the Atlantic for the period covered.

We further compare the above results with a longer record of storm sizes in the NATL (Fig. 5) and WPAC (Fig. 6) to show how the above tendencies fit within a larger context. In the NATL, the period examined is from 1988 to 2021, which covers the availability of EBT data. In the WPAC, a data set of *R*30 and *R*50 from 1977 to 2020 was calculated from data provided by JMA RSMC Tokyo - Typhoon Center. Since the alternative WPAC data set is based fundamentally on different data from an independent source, it is wise to assess how well it corresponds with the IBTrACS data during the period of overlap. As such, we have computed the correlation coefficient between *AR*30 (Fig. 6(b)) and *AR*34 (Fig. 4(b)) for the period of overlap. The correlation coefficients for TS, HT, and ALL are respectively 0.54, 0.47, and 0.51. All of these values are statistically significant with at least 95% confidence.

The extended NATL data set exhibits both similarities and differences when compared against more recent data, by comparing Fig. 5 with Figs. 3(a), 3(d), 4(a), 4(d), and 4(g). Both data sets exhibit a significant increase in *RMW* for TS (+5.80 nm/decade) and ALL (+4.22 nm/decade), though a negative linear tendency in *RMW* is seen in the extended data set but not the more recent data for HT (Fig. 5(a) v.s. Fig. 3(a)). However, we consider this tendency to be suspicious because it appears to reflect a sudden change centered around the year 2001; before that, the *RMW* was relatively constant near 30 nm, and after that it was relatively constant around 20 nm. This may be caused by a change in measurement method or instrument availability. The linear tendencies of *AR*34 for TS (+7.37 nm/decade) are also significant in the extended data set but not in the recent data (Fig. 5(b) v.s. Fig. 4(a)). In addition, quadratic fits to the extended NATL data set exhibit much higher significance than do the quadratic fits to the shorter 2001−2021 data. This suggests that the extended data set better captures decadal-scale forcing in the NATL than does the more recent data. Consistent conclusions are found for the TC area changes over the NATL (Figs. 5(c)–5(e)).

For the WPAC, the major difference between the extended and recent WPAC data sets is that the increasing tendency of *AR*30 of TS is insignificant from 1977 to 2020 in the extended data set but significant from 2001 to 2021 (Fig. 6(b) v.s. Fig. 4(b)). On the other hand, the significant decreasing tendency of AR50 (−5.63 nm/decade) is consistent with that of *RMW* for WPAC HT (Fig. 6(a) v.s. Fig. 3(b)). Consistent conclusions are found for the TC area changes over the WPAC (Figs. 6(c)–6(f)). In a previous publication, Shou et al. (2021), by estimating the

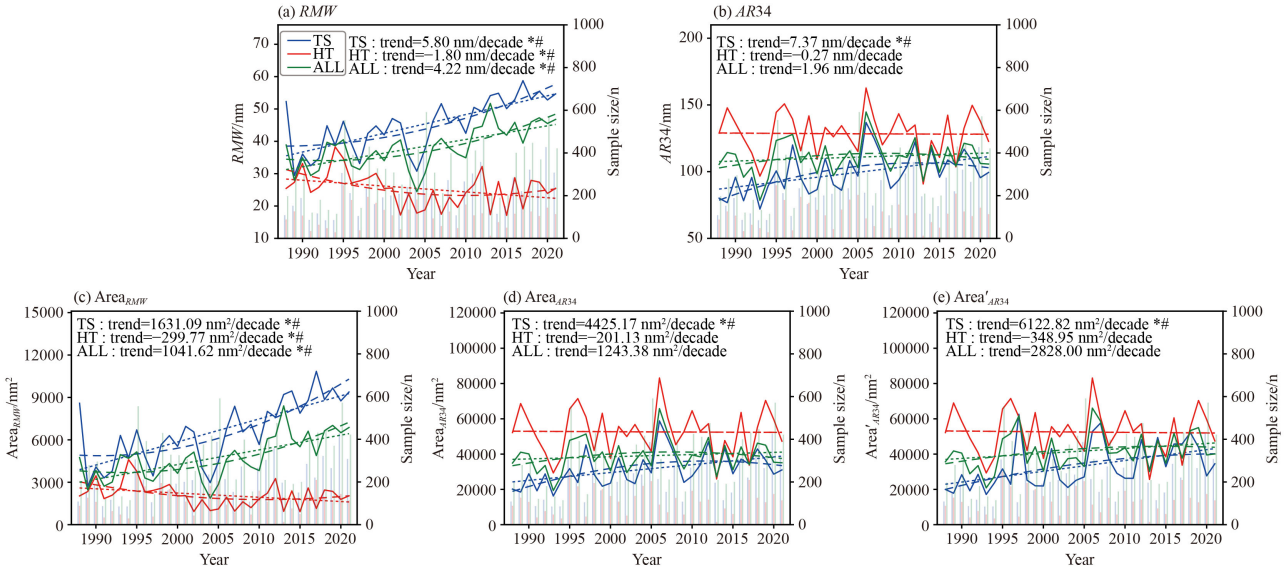

Fig. 5 Time series of the (a) *RMW* (unit: nm), (b) *AR*34 (unit: nm), (c) Area$_{MWR}$ (unit: nm^2), (d) Area$_{AR34}$ (unit: nm^2), and (e) Area′$_{AR34}$ (unit: nm^2) from 1988 to 2021 over the NATL. The blue, red, and green solid curves indicate the TS, HT, and ALL storms, respectively. Dotted and dashed lines respectively show the best fit linear and quadratic tendencies. The blue, red, and green bars indicate the sample sizes of the TS, HT, and ALL storms of each year. The linear tendency values are shown in the figure legends, with the asterisk (*) and hashtag (#) symbols denoting linear and quadratic fittings that are statistically significant with at least 90% confidence level. Results are based on the EBT data set.

TC *RMW* with the model from Chavas et al. (2015), showed a significant decreasing trend in the inner core sizes of WPAC TCs with maximum sustained wind speed larger than 34 kt, from 1981 to 2016. Despite using a different definition of TC *RMW*, the results of Fig. 6 are consistent with that of Shou et al. (2021), in terms that the *AR*50 and Area$_{AR50}$ of the WPAC decreases significantly from 1977 to 2020 (Figs. 6(a) and 6(c)). However, the decreasing trend of the WPAC inner core size is statistically insignificant in the study period (2001–2021) of this study. This may be due to a decadal shift of the TC size series since 2001, as shown in both Fig. 6(a) and also in Fig. 2 of Shou et al. (2021).

3.3 Changes in storm sizes for landfalling TCs

While discussing TC variability, it is particularly important to respectively examine the differences between landfalling and non-landfalling TCs because the TC characteristics significantly vary between these two categories and the public, as well as risk managers, are more concerned about the landfalling TCs. Hence, in the following two subsections, we repeat the above analyses about the changes in TC size by dividing all the samples into 1) landfalling and 2) non-landfalling TCs.

Figure 7 shows the size changes of the inner core (based on *RMW*) of the landfalling TCs. Over the NATL, it is observed that the landfalling TS *RMW* has been increasing significantly (+12.2 nm/decade) since 2001, while that of HT exhibits an insignificant tendency (Fig. 7(a)). For the WPAC, the inner core size change of landfalling HT (−2.60 nm/decade) is opposite to that of landfalling TS (+4.00 nm/decade) (Fig. 7(b)), being consistent with that shown in Fig. 3(b). Meanwhile, for the EPAC, the changes in *RMW* of both landfalling HT and TS are insignificant (Fig. 7(c)). Further, Fig. 8 gives the size changes of the outer core (based on *AR*34) of the landfalling TCs. Results show that the changes of *AR*34 of NATL TS, NATL HT, WPAC TS, WPAC HT and EPAC TS are all insignificant. Exceptions are found for that of EPAC HT which decreases by 24.3 nm/decade.

As a result, from 2001 to 2021, for the NATL, the TS inner core has been expanding without apparent changes in its outer core; meanwhile, both the inner and outer cores of the HT do not show significant changes (Figs. 7(d), 8(d), and 8(g)). For the WPAC, both the inner and outer cores of TSs have expanded significantly; in contrast, the HT inner core has shrunk since 2001 without significant changes in its outer core size (Figs. 7(e), 8(e), and 8(h)). For the EPAC, both the inner and outer cores of TSs have no significant changes; however, the HT outer core has shrunk since 2001 without significant changes in its inner core size (Figs. 7(f), 8(f), and 8(i)).

3.4 TC size change for non-landfalling TCs

Similarly, the changes in storm sizes of non-landfalling TCs are also analyzed and given here. Figure 9 shows the size changes of the inner core (based on *RMW*) of the non-landfalling TCs. The results are overall consistent with those of all TCs (Fig. 3(a)). Additionally, over the NATL, the TS *RMW* has been increasing significantly

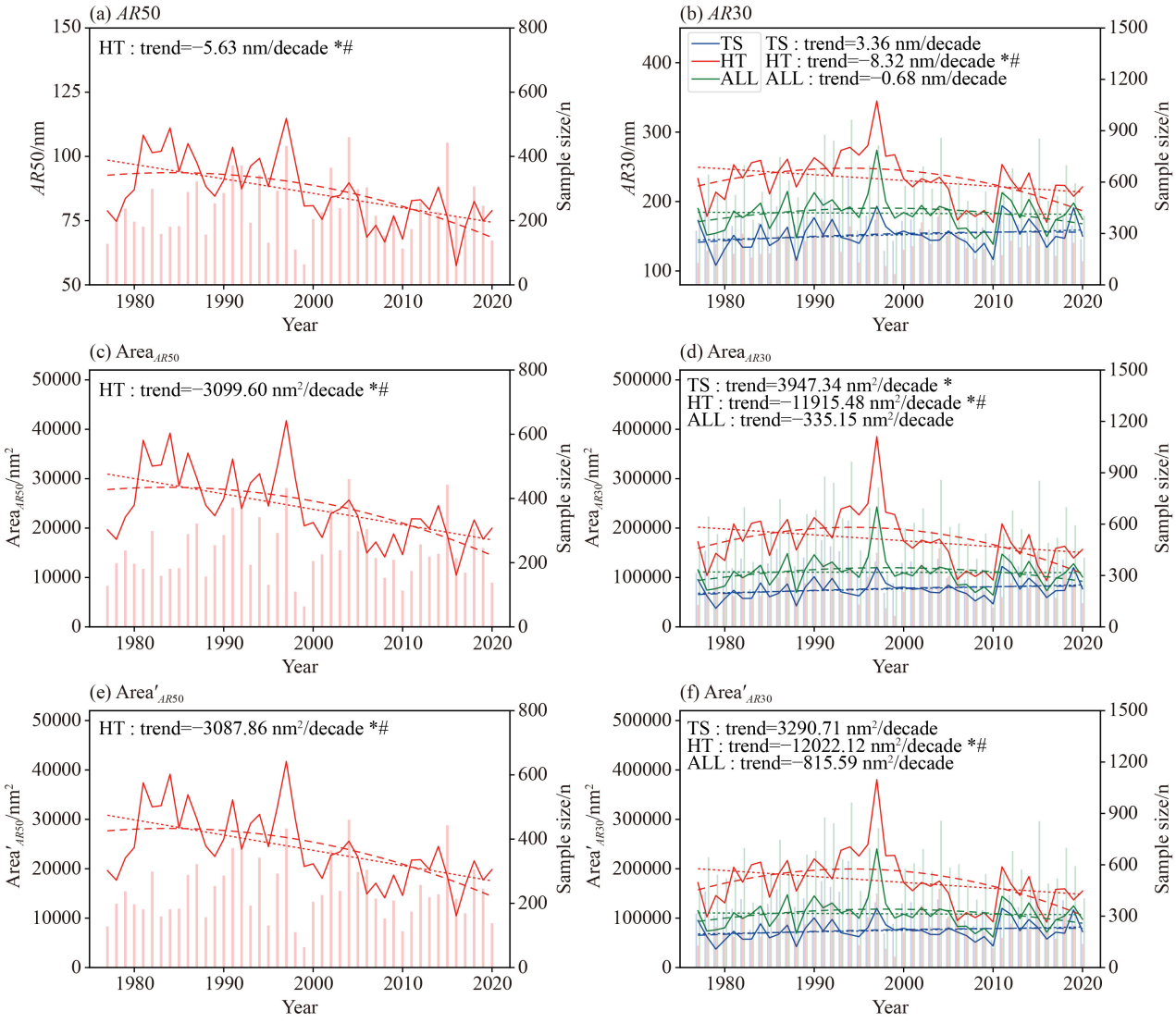

Fig. 6 Time series of the (a) *AR*50 (unit: nm), (b) *AR*34 (unit: nm), (c) Area$_{AR50}$ (unit: nm^2), (d) Area′$_{AR50}$ (unit: nm^2), (e) Area$_{AR34}$ (unit: nm^2), and (f) Area′$_{AR34}$ (unit: nm^2) from 1977 to 2020 over the WPAC. The blue, red, and green solid curves indicate the TS, HT, and ALL storms, respectively. Dotted and dashed lines respectively show the best fit linear and quadratic tendencies. The blue, red, and green bars indicate the sample sizes of the TS, HT, and ALL storms of each year. The linear tendency values are shown in the figure legends, with the asterisk (*) and hashtag (#) symbols denoting linear and quadratic fittings that are statistically significant with at least 90% confidence level. Results are based on the JMA RSMC best track data.

(+5.35 nm/decade) since 2001, while that of HT exhibits an insignificant tendency (Fig. 9(a)). For the WPAC, the inner core size change of non-landfalling TS is significantly positive (+5.92 nm/decade) but that of HT is insignificant (Fig. 9(b)). For the EPAC, the changes in *RMW* of both landfalling HT and TS are insignificant (Fig. 9(c)).

The size changes of the outer core (based on *AR*34) of the non-landfalling TCs are plotted in Fig. 10. Interestingly, the results are overall consistent with those of landfalling TCs (Fig. 8). It is found that the changes of *AR*34 of non-landfalling NATL TS, NATL HT, WPAC HT, and EPAC TS are all insignificant. Similar to landfalling TCs, exceptions are found for that of WPAC TS which increases by 13.1 nm/decade, and that of EPAC HT which decreases by 12.4 nm/decade.

As a result, from 2001 to 2021, for the NATL, the TS inner core has been expanding significantly without apparent changes in its outer core size; meanwhile, both the inner and outer cores of the HT do not show significant changes (Figs. 9(d), 10(d), and 10(g)). For the WPAC, both the inner and outer cores of TSs have expanded significantly; in contrast, the HT has no significant changes in the sizes of its inner and outer cores (Figs. 9(e), 10(e), and 10(h)). For the EPAC, both the inner and outer cores of TSs have no significant changes; however, the HT outer core has shrunk since 2001 without significant changes in its inner core size

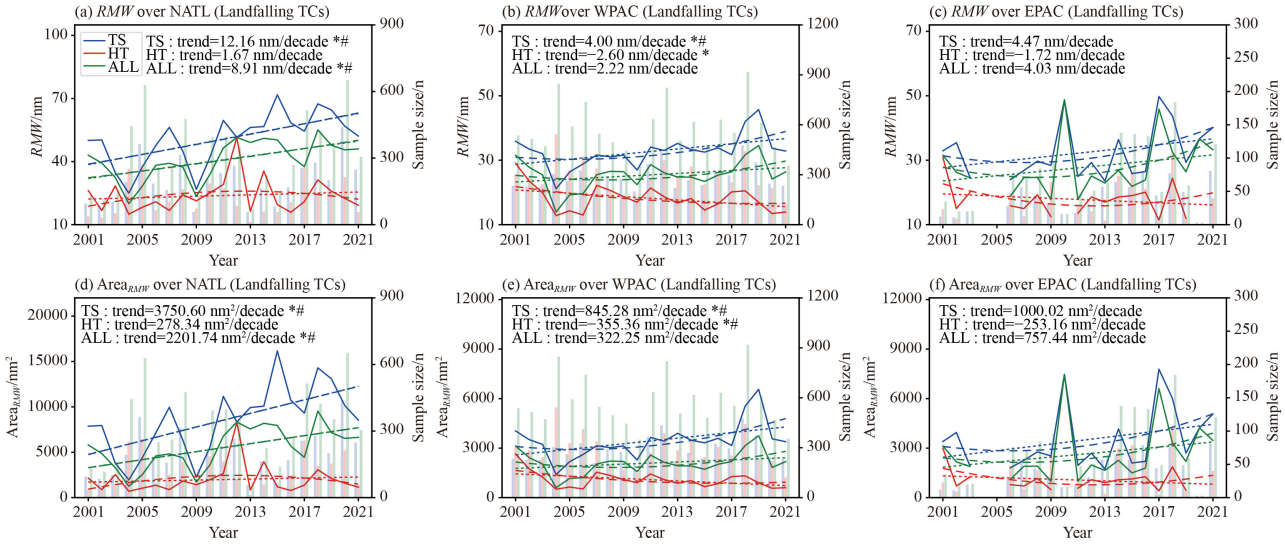

Fig. 7 Same as Fig. 3, except for landfalling TCs only.

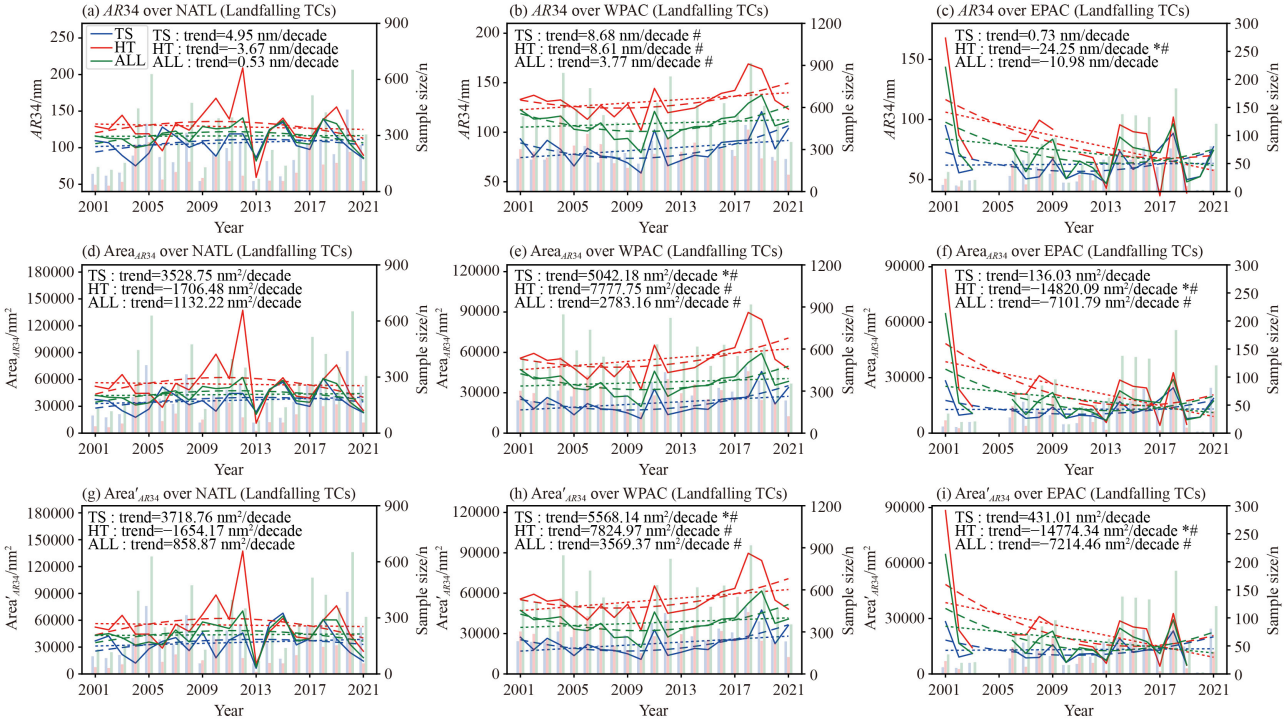

Fig. 8 Same as Fig. 4, except for landfalling TCs only.

(Figs. 9(e), 10(e), and 10(h)), being consistent to the landfalling EPAC HTs.

4 Summary

Storm size plays a very important role in cyclone forecasts, storm surge studies, and the cyclone climate and its changes (Rotunno and Emanuel, 1987; Irish et al., 2008; Chen et al., 2011; Emanuel, 2012; Stern et al., 2015; Xu et al., 2016). In this study, we used linear and quadratic curve fittings to investigate the recent tendencies of TC size based on *RMW* and *AR*34 over the NATL, WPAC, and EPAC basins from 2001 to 2021. Results show that there is a great inter-basin variability among the changes in TC size. The major changes found are summarized below and in Fig. 11.

1) For the NATL, overall, both the inner and outer cores of all TCs have been expanding but those of HTs do not show significant changes. However, while considering landfalling TCs alone, the TS inner core has been expanding without apparent changes in its outer core; meanwhile, the HT does not show significant changes.

2) For the WPAC, both the inner core of landfalling

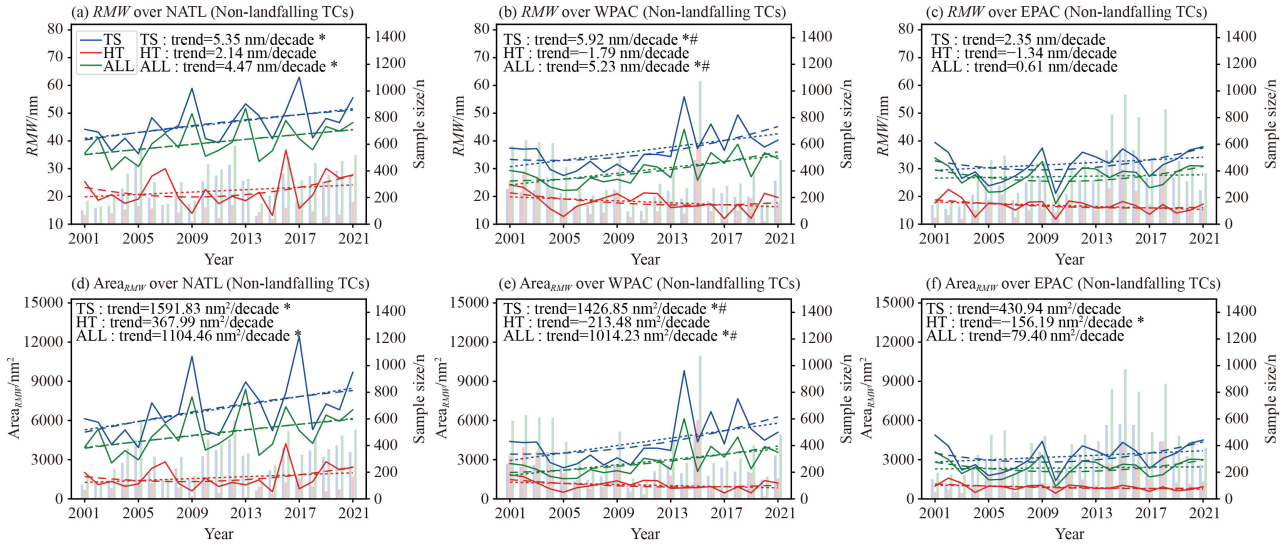

Fig. 9 Same as Fig. 3, except for non-landfalling TCs only.

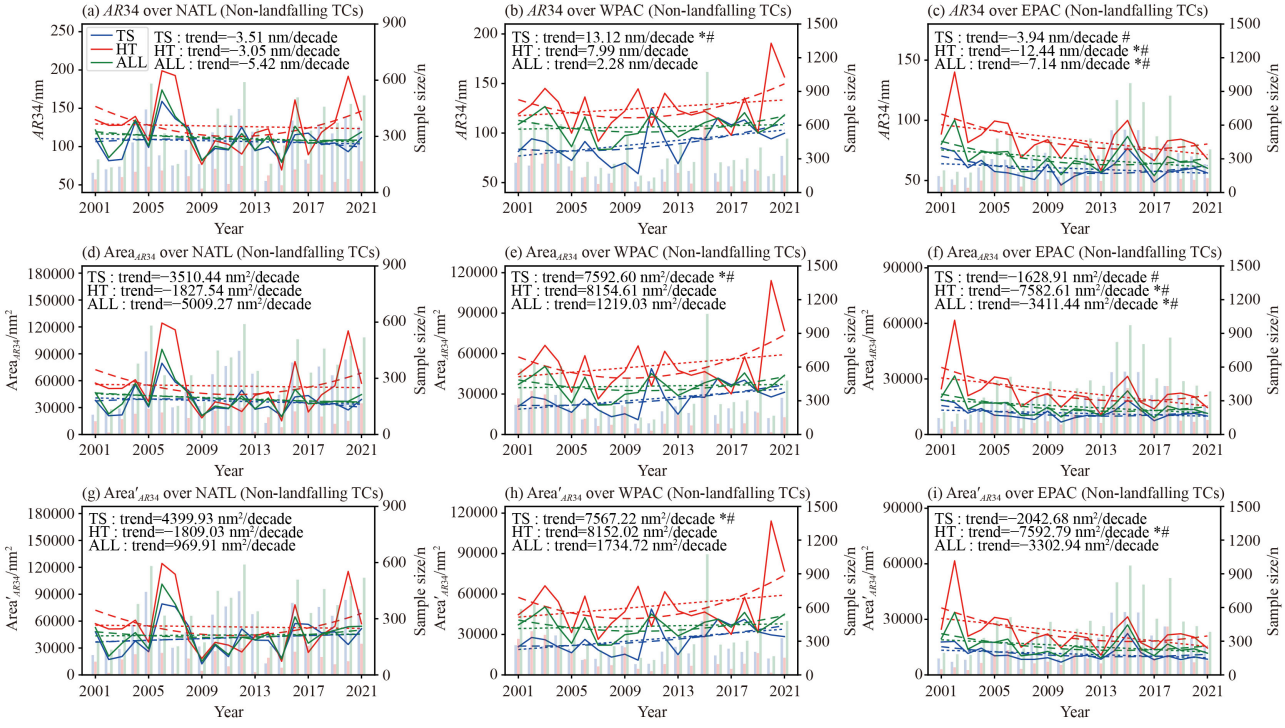

Fig. 10 Same as Fig. 4, except for non-landfalling TCs only.

TSs has expanded significantly while the outer core has an insignificant positive change; in contrast, the HT inner core has shrunk without significant changes in its outer core size. However, for non-landfalling TCs, while the TS size shows expansion in both inner and outer cores, there are no significant changes in both the inner and outer cores of the HT.

3) For the EPAC, regardless of whether the TCs make landfall, both the inner and outer cores of TSs have no significant changes; however, the HT outer core has become smaller without significant changes in its inner core size.

Overall, the inner cores of TSs have either become larger or exhibited no significant changes in all the three basins, while those of HTs mostly get smaller or remain similar. Meanwhile, comparatively large inter-basin differences are observed for the TC outer core sizes, and the sizes of landfalling TCs. Particularly, a significant decrease in landfalling HT outer core size is observed over the EPAC; in contrast, significant increases in landfalling TS inner core size is found over the NATL and WPAC (Fig. 11).

The statistical significances of the two storm size estimations, namely *RMW* and *AR*34, are quite different,

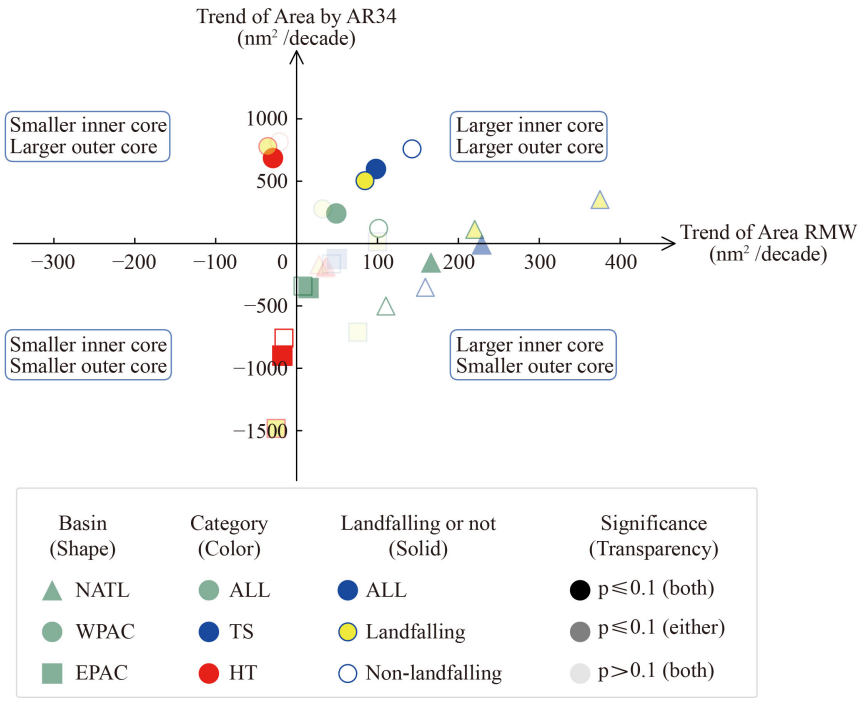

Fig. 11 A scatter plot summarizing the linear tendencies of TC size over different basins from 2001 to 2021. Triangles, circles, and squares respectively denote TCs over the NATL, WPAC, and EPAC. Green, blue and red colors respectively denote ALL, TS, and HT. Solid circles denote all TCs without considering whether they make landfall, while centers filled with yellow and white colors respectively denote landfalling and non-landfalling TCs. Symbols with 100% opacity denote the tendencies of both Area_{AR34} and Area_{RMW} are significant at the 90% confidence level; that with 50% opacity denote only one of the two linear tendencies is significant at the 90% confidence level; that with 10% opacity denote both linear tendencies are statistically insignificant.

with *RMW* having more significant tendencies than *AR*34. This could suggest *AR*34 being influenced more by environmental conditions, such as interdecadal variability, thus having more complex characteristics. The parameter *RMW* is more representative of storm size reflecting forcing strength, such as SST, with a better linear tendency and decadal scale variability. The quadratic fitting also increases the confidence level of statistical significance, particularly in the WPAC and EPAC basins where the decadal scale variability accounts for a significant part of the size variation. However, since only 21 years data were applied in this study, which is too short to extract interdecadal signals, one should be aware when interpreting the quadratic curves.

Acknowledgments This work is supported by the Guangdong Province Introduction of Innovative R&D Team Project China (No. 2019ZT08G669), the Guangdong Basic and Applied Basic Research Foundation (No. 2020A1515110275), the Guangdong Science and Technology Key Project (No. 21080208). We would also like to thank the HWRF team of NOAA/NCEP/EMC for making this study possible.

Competing Interests The authors declare that they have no competing interests.

References

Barbosa S M (2011). Testing for deterministic trends in global sea surface temperature. J Clim, 24(10): 2516–2522

Carrasco C, Landsea C, Lin Y (2014). The influence of tropical cyclone size on its intensification. Weather Forecast, 29(3): 582–590

Chan K T F, Chan J C L (2015). Global climatology of tropical cyclone size as inferred from QuikSCAT data. Int J Climatol, 35(15): 4843–4848

Chavas D R, Emanuel K A (2010). A QuikSCAT climatology of tropical cyclone size. Geophys Res Lett, 37(18): L18816

Chavas D R, Lin N, Emanuel K (2015). A model for the complete radial structure of the tropical cyclone wind field. Part I: Comparison with observed structure. J Atmos Sci, 72(9): 3647–3662

Chen D Y C, Cheung K K W, Lee C S (2011). Some implications of core regime wind structures in western North Pacific tropical cyclones. Weather Forecast, 26(1): 61–75

Demuth J, DeMaria M, Knaff J A (2006). Improvement of advanced microwave sounder unit tropical cyclone intensity and size estimation algorithms. J Appl Meteorol Climatol, 45(11): 1573–1581

Doocy S, Dick A, Daniels A, Kirsch T D (2013). The human impact of tropical cyclones: a historical review of events 1980–2009 and systematic literature review. PLoS Curr, doi: 10.1371/currents.dis.2664354a5571512063ed29ed29d25ffbce74

Emanuel K (2005). Increasing destructiveness of tropical cyclones over the past 30 years. Nature, 436(7051): 686–688

Emanuel K A (2012). Self-stratification of tropical cyclone outflow. Part II: implications for storm intensification. J Atmos Sci, 69(3):

988–996

Emanuel K A, Sobel A (2013). Response of tropical sea surface temperature, precipitation, and tropical cyclone–related variables to changes in global and local forcing. J Adv Model Earth Syst, 5(2): 447–458

Emanuel K A, Sundararajan R, Williams J (2008). Hurricanes and global warming: results from downscaling IPCC AR4 simulations. Bull Am Meteorol Soc, 89(3): 347–368

Grinsted A, Moore J C, Jevrejeva S (2012). Homogeneous record of Atlantic hurricane surge threat since 1923. Proc Natl Acad Sci USA, 109(48): 19601–19605

Irish J L, Resio D T, Ratcliff J J (2008). The influence of storm size on hurricane surge. J Phys Oceanogr, 38(9): 2003–2013

Islam M R, Lee C Y, Mandli K T, Takagi H (2021). A new tropical cyclone surge index incorporating the effects of coastal geometry, bathymetry and storm information. Sci Rep, 11(1): 16747

Islam M R, Satoh M, Takagi H (2022). Tropical cyclones affecting Japan central coast and changing storm surge hazard since 1980. J Meteorol Soc Jpn, 100(3): 493–507

Jin F F, Boucharel J, Lin I I (2014). Eastern Pacific tropical cyclones intensified by El Niño delivery of subsurface ocean heat. Nature, 516(7529): 82–85

Kimball S K, Mulekar M S (2004). A 15-year climatology of North Atlantic tropical cyclones. Part I: Size parameters. J Climate, 17: 3555–3575

Kishimoto K (2008). Revision of JMA's early stage Dvorak analysis and its use to analyze tropical cyclones in the early developing stage. RSMC Tokyo-Typhoon Center Technical Review, 10: 1–12

Klotzbach P J (2006). Trends in global tropical cyclone activity over the past twenty years (1986–2005). Geophys Res Lett, 33(10): L10805

Klotzbach P J, Bell M M, Bowen S G, Gibney E J, Knapp K R, Schreck C J (2020). Surface pressure a more skillful predictor of normalized hurricane damage than maximum sustained wind. Bull Am Meteorol Soc, 101(6): E830–E846

Klotzbach P J, Landsea C W (2015). Extremely intense hurricanes: revisiting Webster et al. (2005) after 10 Years. J Clim, 28(19): 7621–7629

Knaff J A, Longmore S P, Molenar D A (2014). An objective satellite-based tropical cyclone size climatology. J Clim, 27(1): 455–476

Knapp K R, Kruk M C, Levinson D H, Diamond H J, Neumann C J (2010). The International Best Track Archive for Climate Stewardship (IBTrACS): unifying tropical cyclone best track data. Bull Am Meteorol Soc, 91(3): 363–376

Kossin J P (2017). Hurricane intensification along United States coast suppressed during active hurricane periods. Nature, 541(7637): 390–393

Landsea C W, Franklin J L (2013). Atlantic hurricane database uncertainty and presentation of a new database format. Mon Weather Rev, 141(10): 3576–3592

Landsea C W, Pielke Jr R A, Mestas-Nunez A M, Knaff J A (1999). Atlantic basin hurricanes: indices of climatic changes. Climatic Change, 42(1): 89–129

Landsea C W, Vecchi G A, Bengtsson L, Knutson T R (2010). Impact of duration thresholds on Atlantic tropical cyclone counts. J Clim, 23(10): 2508–2519

Lin Y, Zhao M, Zhang M (2015). Tropical cyclone rainfall area controlled by relative sea surface temperature. Nat Commun, 6(1): 6591

Martinez-Sanchez J N, Cavazos T (2014). Eastern Tropical Pacific hurricane variability and landfalls on Mexican coasts. Clim Res, 58(3): 221–234

McDonald J H (2014). Handbook of Biological Statistics (3rd ed.). Baltimore: Sparky House Publishing

Mei W, Xie S P, Primeau F, McWilliams J C, Pasquero C (2015). Northwestern Pacific typhoon intensity controlled by changes in ocean temperatures. Sci Adv, 1(4): e1500014

Merrill R T (1984). A comparison of large and small tropical cyclones. Mon Weather Rev, 112(7): 1408–1418

Nekkali Y S, Osuri K K, Das A K (2022). Numerical modeling of tropical cyclone size over the Bay of Bengal: influence of microphysical processes and horizontal resolution. Meteorol Atmos Phys, 134(4): 72

Rotunno R, Emanuel K A (1987). An air–sea interaction theory for tropical cyclones. Part II: evolutionary study using a nonhydrostatic axisymmetric numerical model. J Atmos Sci, 44(3): 542–561

Shen W (2006). Does the size of hurricane eye matter with its intensity? Geophys Res Lett, 33(18): L18813

Shou H R, Li T, Sun Y, Wang L, Liu J (2021). Decreasing trend of western North Pacific tropical cyclone inner-core size over the past decades. J Meteorol Res, 35(4): 635–645

Stern D P, Vigh J L, Nolan D S, Zhang F (2015). Revisiting the relationship between eyewall contraction and intensification. J Atmos Sci, 72(4): 1283–1306

Takagi H, Wu W (2016). Maximum wind radius estimated by the 50 kt radius: improvement of storm surge forecasting over the western North Pacific. Nat Hazards Earth Syst Sci, 16(3): 705–717

Wang B, Yang Y, Ding Q H, Murakami H, Huang F (2010). Climate control of the global tropical storm days (1965–2008). Geophys Res Let, 37: L07704

Webster P J, Holland G J, Curry J A, Chang H R (2005). Changes in tropical cyclone number, duration, and intensity in a warming environment. Science, 309(5742): 1844–1846

Xu J, Wang Y (2010a). Sensitivity of the simulated tropical cyclone inner-core size to the initial vortex size. Mon Weather Rev, 138(11): 4135–4157

Xu J, Wang Y (2010b). Sensitivity of tropical cyclone inner-core size and intensity to the radial distribution of surface entropy flux. J Atmos Sci, 67(6): 1831–1852

Xu J, Wang Y, Tan Z M (2016). The relationship between sea surface temperature and maximum intensification rate of tropical cyclones in the North Atlantic. J Atmos Sci, 73(12): 4979–4988